ELSEVIER

Journal of Nuclear Materials 253 (1998) 219–226

journal of nuclear materials

Compatibility of insulating ceramic with liquid breeders

Takayuki Terai [a,*], Takaaki Mitsuyama [b], Toshiaki Yoneoka [b], Satoru Tanaka [b]

[a] *Engineering Research Institute, University of Tokyo, 2-11-16, Yayoi, Bunkyo-ku, Tokyo 113, Japan*
[b] *Department of Quantum Engineering and Systems Science, University of Tokyo, 7-3-1 Hongo, Bunkyo-ku, Tokyo 113, Japan*

Abstract

The compatibility of candidate materials for insulating ceramic coatings (Y_2O_3, Al_2O_3, MgO, $3Al_2O_3$–MgO, AlN (60%)–BN (40%) and BN) with liquid metal breeders such as metallic lithium and lithium–lead alloy (Li17–Pb83) was investigated at 773 K up to 5 Ms by monitoring weight change, structural integrity and electrical resistivity. Oxides such as Al_2O_3 and $3Al_2O_3$–MgO were severely corroded and dissolved or broken by lithium, while MgO was corroded uniformly with a moderate rate (e.g. 27 μm for 4.8 Ms). The most thermodynamically stable Y_2O_3 was less corroded and showed a slight decrease in electrical resistivity due to the formation of non-stoichiometric Y_2O_{3-x}. On the other hand, no oxides were corroded at all by Li17–Pb83. These results were in good agreement with thermodynamical predictions, and most of the oxides maintained their high electrical resistivity even after the corrosion test in liquid lithium. Nitrides such as AlN–BN and BN were corroded by lithium and became fragile because impurities included in the specimens were dissolved in the lithium. © 1998 Elsevier Science B.V.

1. Introduction

In D–T fusion reactor designs, a liquid blanket concept is a promising one to realize a DEMO fusion reactor system of high power density, because it has advantages such as the continuous replacement of breeders for reprocessing, no radiation damage for breeders, a larger tritium breeding ratio (TBR), a simpler blanket structure and better thermal transfer than a solid blanket concept. On the other hand, it has several critical issues: (1) a large MHD pressure drop requires a large pump power, in particular, for self-cooled designs, (2) liquid breeders have a high chemical reactivity including low compatibility with structural materials and (3) a large amount of tritium may leak to the environment due to permeation through structural materials, particularly in a Li17–Pb83 blanket design.

In order to solve these critical issues, the placement of a ceramic coating on the inner surface of the coolant ducts in the blanket is proposed [1]. The coating should have a high electrical resistance, high corrosion resistance, low tritium permeability and a high thermomechanical integrity. Moreover, these properties should be maintained in the actual blanket conditions including a high radiation field, large production rate of hydrogen and helium atoms by transmutation, high temperature, large temperature gradient, thermal cycle, high magnetic and electric field and the presence of reductive liquid metals.

In order to determine what is the most promising material for ceramic coating, data on the compatibility with liquid breeders as well as the electrical resistivity change in the presence of liquid breeders are required. In general, the compatibility of ceramic insulators with liquid metals should be considered from the perspectives of thermodynamics and kinetics. Up to now, there have been some extensive corrosion experiments carried out on oxides (SiO_2, TiO_2, Y_2O_3, YSZ, Cr_2O_3, Al_2O_3, MgO, BeO, $Y_3Al_2O_{12}$, etc.), nitrides (Si_3N_4, AlN, BN, TiN, etc.) and carbides (SIC, etc.) in lithium. It was reported that SiC, Y_2O_3, AlN, MgO, BeO, etc. remain intact in liquid lithium at 673–723 K. From these results and other properties such as fabricability, etc., AlN has been proposed as a primary candidate material for ceramic coating in the presence of liquid lithium [2]. On the other hand, Al_2O_3 was proposed as a candidate material for ceramic coating in the presence of Li17–Pb83 because of its thermochemical stability in Li17–Pb83 and its very high electrical resistivity [3].

* Corresponding author. Tel.: +81-3 381 2111; fax: +81-3 5800 6824; e-mail: tera@starling.t.u-tokyo.ac.jp.

PII S0022-3115(97)00334-6

The corrosion behavior of ceramics is often strongly influenced by the additives, impurities and morphology (porosity, grain boundary structure, etc.) of specimens. However, the effects and the roles of these parameters have not yet been elucidated. Electrical resistivity changes due to corrosion is also a concern for an insulating coating. In this study, oxides such as yttria (Y_2O_3), corundum (Al_2O_3), magnesium oxide (MgO) and spinel ($MgAl_2O_4$), and nitrides such as aluminum nitride and boron nitride mixture (AlN (60%)–BN (40%)) and boron nitride (BN) were examined in compatibility with liquid breeders such as molten lithium and Li17–Pb83, focusing on the effects of impurities and morphology. Some specimens of each materials were immersed in the liquid breeders and their changes in morphology, weight and electrical resistivity were investigated.

2. Experimental

The liquid breeder materials used in the examination were lithium (whose purity was more than 99.9%) and Li17–Pb83 (which was prepared from reagent grade lithium and lead under inert atmosphere). The oxide specimens were poly-crystalline yttria (Y_2O_3, $17 \times 17 \times 1$ mm), single-crystalline corundum (Al_2O_3, 20 mm in diameter $\times$ 1 mm), single-crystalline magnesium oxide (MgO, $20 \times 20 \times 1$ mm) and single-crystalline spinel having the composition of $3Al_2O_3$–MgO ($20 \times 20 \times 1$ mm) instead of stoichiometric compound $MgAl_2O_4$, and the nitride specimens were sintered aluminum nitride–boron nitride mixture (AlN (60%)–BN (40%), 21 mm in diameter $\times$ 1 mm) and sintered boron nitride (BN, 20 mm in diameter $\times$ 1 mm).

The experimental apparatus is shown in Fig. 1. The liquid breeder material used in the corrosion test was about 20–30 g per batch. In a glove box with Ar gas, the crucible loaded with specimens and liquid breeder material was set in a heating container made of AISI type 316 stainless steel. During the exposure at 773 K for up to 5 Ms, Ar gas was allowed to flow over the liquid metal. After the corrosion test, each specimen was taken out of the crucible, the lithium metal adhering to the corroded specimens was cleansed with water and ethyl–alcohol and the Li17–Pb83 was cleansed with a mixed solution of an acetic acid, hydrogen peroxide, water and ethyl–alcohol. The dimension and the weight of each specimen were then measured. The chemical composition and the compositional image of a cross section of each specimen were analyzed by EPMA and the chemical phase contained in each specimen was determined by XRD. Electrical conductivity measurements were also carried out at room temperature for each specimen by conventional methods.

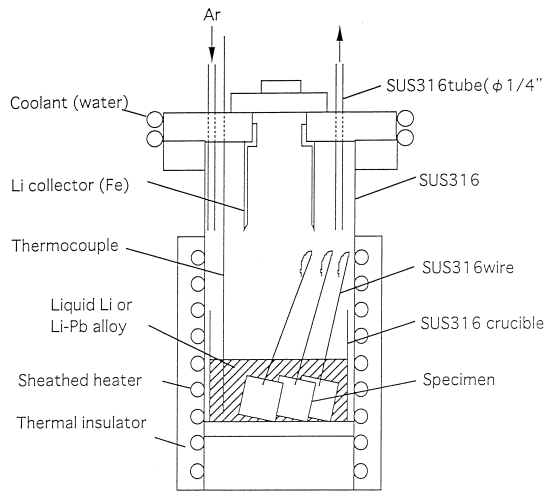

Fig. 1. Experimental apparatus for corrosion experiments.

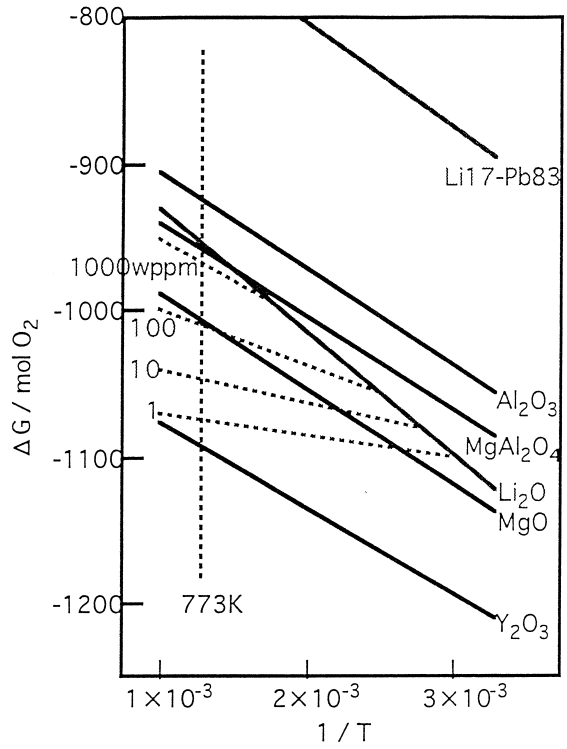

Fig. 2. Free energy of oxide formation for several kinds of metals. Each dashed line means ΔG of the Li–O solution system with the corresponding concentration of O.

3. Results and discussion

3.1. Thermodynamic consideration

The free energies of formation of oxides, nitrides and their solutions with several concentrations [4,5] as a function of reciprocal temperature are shown in Figs. 2 and 3, respectively. Corundum and spinel are less stable than

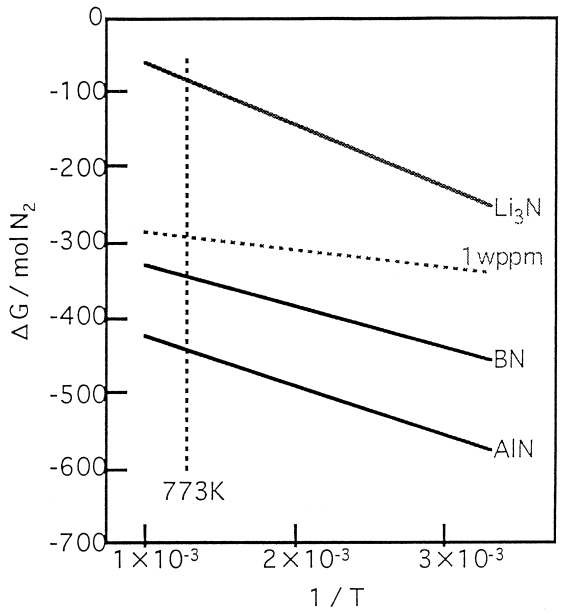

Fig. 3. Free energy of nitride formation for several kinds of metals. The dashed line means ΔG of the Li–N solution system with the N concentration of 1 wppm.

Li_2O. Magnesium oxide is more stable than Li_2O in the case of the Li–Li_2O coexistent system. However, if the oxygen activity is smaller than that of the Li–Li_2O coexistent system (e.g. < 100 wppm at 773 K), magnesium oxide can be reduced in lithium. Yttria is clearly more stable than lithium. Among the nitrides, aluminum nitride and boron nitride are more stable than lithium. From these results, we can estimate thermodynamically what kind of materials are stable in a given condition; yttria and the nitrides are expected to be stable even in the presence of liquid lithium containing very low concentrations of oxygen and nitrogen, respectively.

3.2. Yttria specimens immersed in lithium

All the corroded yttria specimens changed from their initial white color to black, because of the reduction to hypo-stoichiometry, Y_2O_{3-x}. The yttria specimens were, however, almost unchanged in dimension except for a slight increase in thickness (less than 1%). A typical cross-sectional compositional image of a corroded yttria specimen by EPMA is shown in Fig. 4. The dark thin layer observed on the yttria surface was identified as $LiYO_2$ by XRD analysis. It was also suggested that the $LiYO_2$ layer gradually increased its thickness with time [6].

The electrical resistivity obtained by a Cole–Cole's plot at room temperature is shown in Fig. 5. The electrical resistivity decreased from its initial value with time. The reason why the electrical resistivity decreased is that yttria specimens were reduced to the hypo-stoichiometric yttria, which had a lower electrical resistivity than the initial stoichiometric yttria. The value of the electrical resistivity of yttria immersed in lithium for 5.1 Ms was in the order of 10^7 Ω m at room temperature. The electrical conductivity of hypo-stoichiometric yttria reduced by metallic titanium is known to be considerably high at elevated temperatures [7]. The non-stoichiometry of yttria reduced by molten lithium is estimated to be smaller than that by metallic titanium from a thermodynamical consideration. The electrical resistivity of yttria reduced by lithium is, therefore, estimated to be higher than that reduced by titanium. However, considering that any coating made from these ceramics will be used at high temperatures such as 773 K, this value does not seem to be sufficiently large for fusion blanket application.

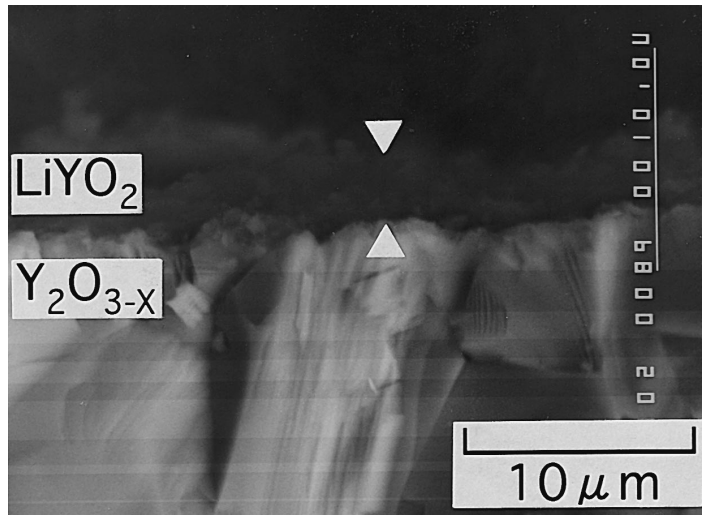

Fig. 4. Typical cross-sectional compositional image of a yttria specimen corroded by lithium for 5.1 Ms at 773 K.

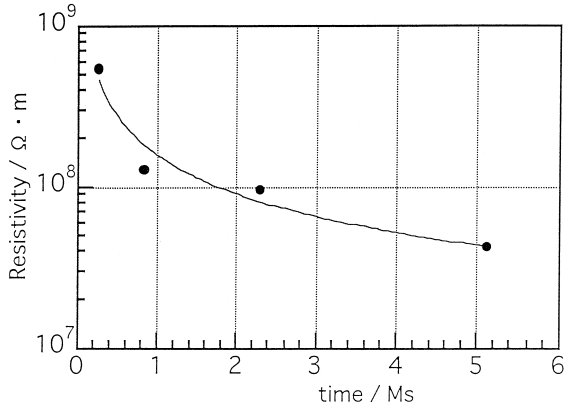

Fig. 5. Temporal change of electrical resistivity of yttria specimen corroded by lithium at 773 K.

3.3. Magnesium oxide specimens immersed in lithium

A photograph of the magnesium oxide specimen corroded for 4.8 Ms is shown in Fig. 6. The corroded magnesium specimens changed from initially transparent to white due to surface roughening with time. The magnesium oxide specimens were locally corroded from their edges and corners. It is well known that a magnesium oxide single crystal cleaves easily and the specimens used here were made by the cleavage method except for the thin edge part (at the top in Fig. 6). Presumably, this corrosion behavior from the edges is caused by fine cleavages at their edges due to mechanical cutting.

The thickness of the specimens was reduced at the most by about 27 μm on the specimens corroded for 4.8 Ms. Except for the edges, the magnesium oxide specimens were, therefore, unchanged in dimension. From a thermodynamic point of view, magnesium oxide is stable against lithium at 773 K in the case of the Li–Li_2O coexistent system, while magnesium oxide is unstable against lithium if the oxygen activity is smaller than that of the Li–Li_2O coexistent system (e.g. 100 wppm), as shown in Fig. 2. The corrosion resistance of magnesium oxide is not sufficient with respect to the postulated conditions of this work. Nevertheless, the electrical resistivity value of the magnesium oxide specimens at room temperature was beyond 10^{10} Ω m, the resolution limit for the measurement.

3.4. Corundum specimens immersed in lithium

The corundum specimens were dissolved in molten lithium within 0.7 Ms. The reason was that corundum is thermodynamically unstable against lithium at 773 K. The formation of stable complex oxides such as $LiAlO_2$ against molten lithium was not observed. It is clearly shown that corundum has no corrosion-resistance to molten lithium.

3.5. Spinel specimens immersed in lithium

The corroded spinel specimens were broken while they were immersed in lithium, in particular a part of the specimens corroded for 0.7 and 2.8 Ms could not be removed from the lithium. A photograph of a spinel specimen corroded for 5.1 Ms is shown in Fig. 7.

The corroded spinel specimens changed from initially transparent to white or grey due to surface roughening.

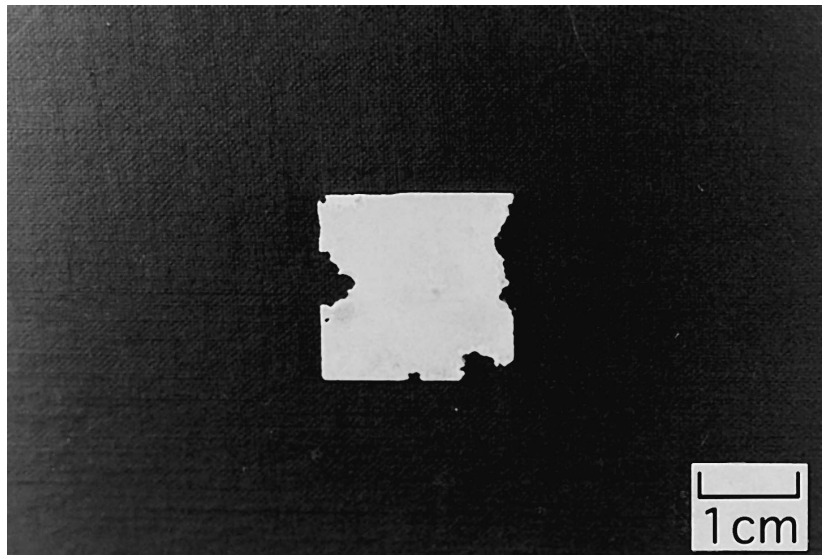

Fig. 6. Photograph of magnesium oxide specimen corroded by lithium for 4.8 Ms at 773 K.

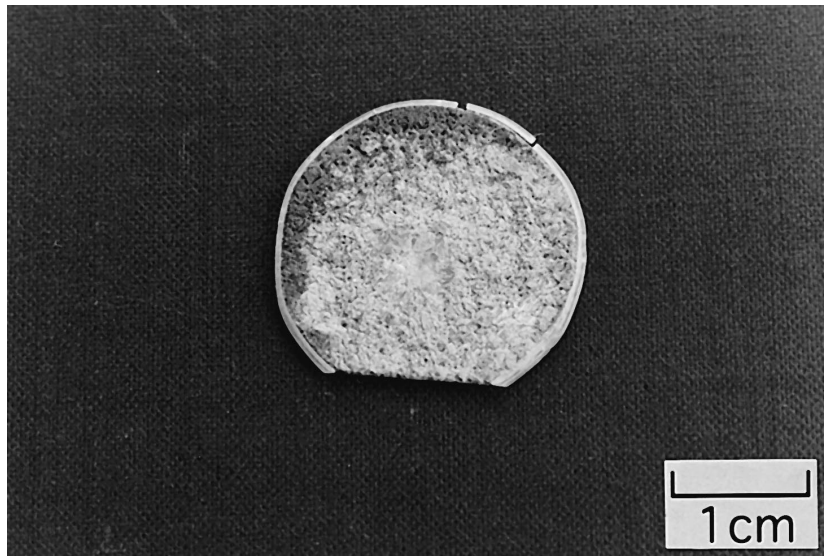

Fig. 7. Photograph of spinel specimen corroded by lithium for 5.1 Ms at 773 K.

The spinel specimens were severely corroded except at the rim and the small center part of the specimens. The surface of the severely corroded part was very rough and the thickness of the part was considerably decreased. The spinel specimens corroded for 2.8 Ms had many small holes through this part. By XRD analysis, magnesium oxide peak was weakly observed on the corroded spinel specimens. From this result, it is presumed that the corrosion of spinel by molten lithium proceeds by penetration of lithium and the dissolution of the alumina component. In addition, the reason for a part being severely corroded is that the alumina component enriched in the part was dissolved in molten lithium.

The magnesium oxide is a corrosion-resistant material with respect to the molten lithium, as mentioned above. The magnesium oxide on a spinel surface is, however, not protective against lithium because it is porous. Nevertheless, the electrical resistivity of the spinel specimen cor-

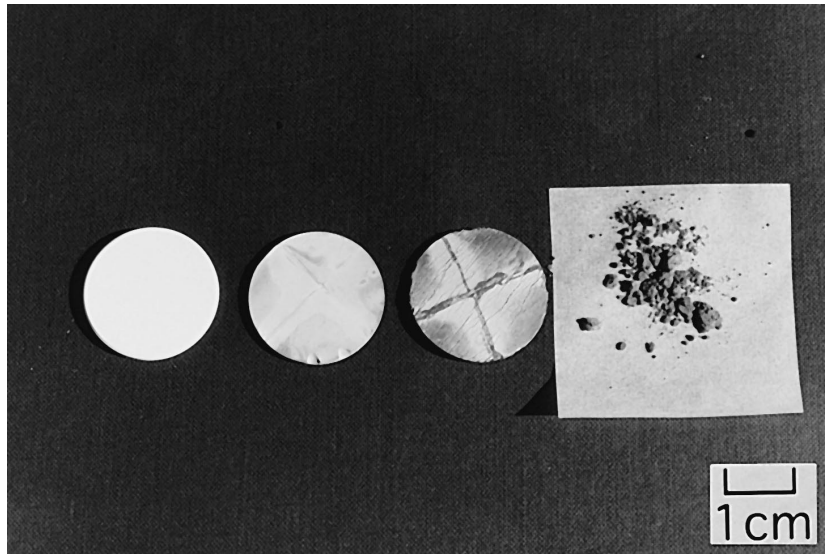

Fig. 8. Photograph of the aluminum nitride–boron nitride mixture specimens uncorroded and corroded by lithium for 0.6, 1.8 and 5.1 Ms by lithium at 773 K.

roded for 1.3 Ms remained beyond the resolution limit of about 10^{10} Ω m.

3.6. All oxide specimens immersed in lithium–lead alloy

None of the oxide specimens (Y_2O_3, Al_2O_3, MgO and $3Al_2O_3$–MgO) immersed in Li17–Pb83 were corroded for up to 5 Ms except for a slight change in surface color. This result is reasonable from a thermodynamic point of view because lithium activity decreased so much (1/10000) in Li17–Pb83. From this point, all the oxides are acceptable as a coating material for the Li17–Pb83 blanket.

3.7. Aluminum nitride–boron nitride mixture specimens immersed in lithium

The used aluminum nitride–boron nitride mixture specimens were sintered AlN (60%)–BN (40%) mixtures containing aluminum oxide as the major impurity (2.7 wt%). The other impurities were Ca < 1000 ppm, Fe < 60 ppm, Si < 100 ppm, C < 600 ppm, Cr < 10 ppm, Mg < 10 ppm, Ni < 10 ppm, etc.

In the experiment, three specimens were immersed in lithium for 0.6, 1.8 and 5.1 Ms. A photograph of uncorroded and corroded AlN–BN specimens is shown in Fig. 8. The AlN–BN specimen corroded for 0.6 Ms did not change in dimensions but slightly changed in its surface color. The specimen corroded for 1.8 Ms had many cracks and significantly changed in its surface color and became curved. The specimen corroded for 5.1 Ms was wetted by lithium when the specimen was taken out from the crucible. When the lithium adhering to the specimen was cleansed with water, the specimen fractured into several pieces as shown in Fig. 8.

The weight of the specimen corroded for 0.6 Ms decreased by 1.8% as compared with its initial value and that

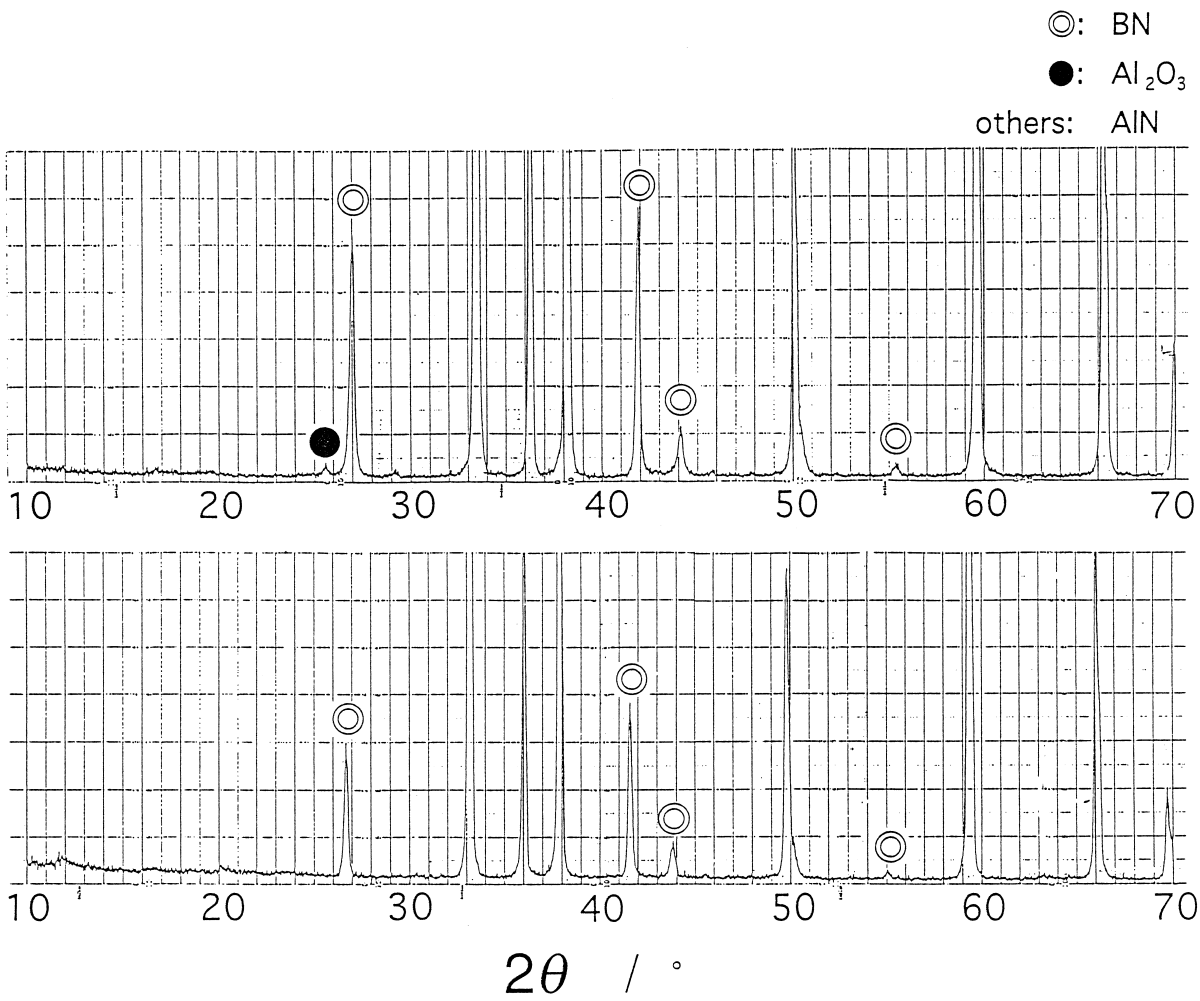

Fig. 9. XRD patterns (Cu K α) of AlN–BN sintered mixture specimen before (top) and after (bottom) corrosion experiment in liquid lithium at 773 K for 1.8 Ms.

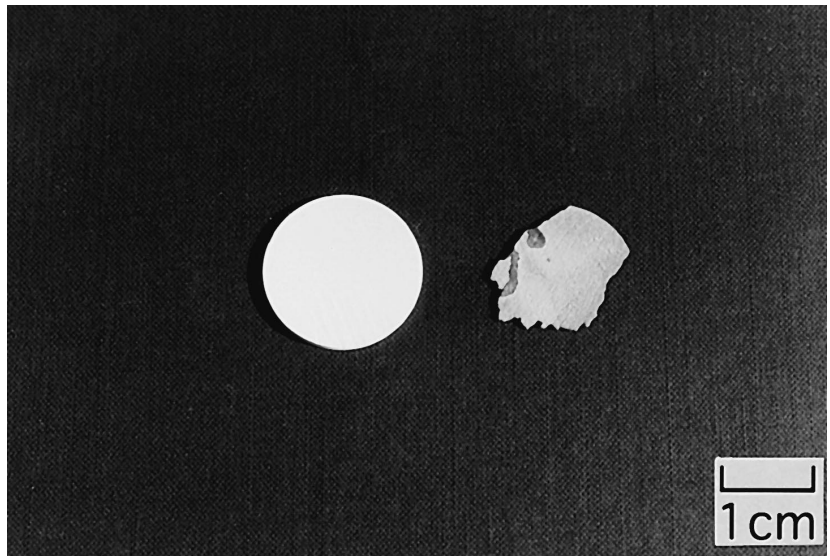

Fig. 10. Photograph of boron nitride specimens uncorroded and corroded by lithium for 0.6 Ms at 773 K.

of the specimen corroded for 1.8 Ms decreased by 9.5%. By XRD analysis, the pattern of aluminum oxide observed in the specimen before the corrosion test was not observed on the corroded AlN–BN specimens, as shown in Fig. 9. The electrical resistivity value of the specimen corroded for 0.6 Ms remained larger than the measurable limit of about 10^{10} Ω m at room temperature. It was estimated that its degradation from the initial value was not significant.

Aluminum nitride and boron nitride are stable against lithium at 773 K thermodynamically and the appearance of the corroded specimens did not change when they were taken out from lithium. Accordingly, it is considered that the matrix of aluminum nitride and boron nitride was not dissolved in lithium, but only aluminum oxide as an impurity (presumably, enriched on grain boundaries) was dissolved in lithium so that the specimens became very fragile. Thus, the specimens corroded for 5.1 Ms, fractured readily in water due to the stresses generated by reaction between water and lithium. It is expected that the AlN–BN specimens containing no impurities that are unstable in lithium will have high corrosion resistance against lithium.

3.8. Boron nitride specimens immersed in lithium

The boron nitride specimens were immersed in lithium for 0.6, 1.8 and 5.1 Ms. A photograph of boron nitride specimens uncorroded and corroded for 0.6 Ms is shown in Fig. 10. The specimen corroded for 0.6 Ms did not change in appearance and was wetted by lithium when the specimen was taken out from the crucible. When the lithium adhering to the specimen was cleansed with water, a part of the specimen fractured and the remaining part was also fragile. The specimens corroded for 1.8 and 5.1 Ms showed a similar behavior. From these results, it is considered that boron nitride was not dissolved in lithium but impurities in the boron nitride were dissolved in lithium, so that the boron nitride became fragile, like the AlN–BN specimens. In some cases, sintered nitrides use B_2O_3 as a sintering aid, which is very soluble in water. However, no B_2O_3

Table 1
Compatibility with liquid lithium at 773 K and electrical resistivity after corrosion experiment

	Y_2O_3	MgO	$3Al_2O_3$-MgO	Al_2O_3	AlN-BN	BN
Compatibility (experiment)	○	△ ~ ○	× ~ △	×	△ ~ ○	△ ~ ○
Compatibility (prediction)	○	△ ~ ○	× ~ △	×	○	○
Electrical resistivity	△	○	○	–	○	○

○; good, △; not recommended, ×; bad.

phase was detected in the specimens in this case by XRD. Therefore, the reason why boron nitride specimens were corroded more severely than AlN–BN specimens may be that boron nitride has better adherence to lithium than AlN–BN mixture.

4. Conclusion

The results obtained in these experiments can be summarized in Table 1, where the compatibility of each compound with lithium at 773 K and the electrical resistivity of each compound after the corrosion experiment are symbolized. Most of the results were in good agreement with a thermodynamic prediction and most of the compounds maintained their high electrical resistivity even in the presence of liquid lithium. However, we should note the following points: (1) in the case of Y_2O_3, a complex compound ($LiYO_2$) and a non-stoichiometric compound (Y_2O_{3-x}) were formed, which was not included in the thermodynamic prediction. (2) In the case of nitrides, some kinds of impurities, such as Al_2O_3, are enriched on grain boundaries and they can be dissolved in liquid lithium, resulting in a decrease in strength of the materials.

References

[1] S. Malang, R. Mattas, Fus. Eng. Des. 27 (1995) 349.
[2] K. Natesan, J. Nucl. Mater. 233–237 (1996) 1403.
[3] H.U. Borgstedt, H. Glassbrenner, J. Nucl. Mater. 27 (1995) 659.
[4] The Japan Society of Calorimetry and Thermal Analysis, MALT (Materials oriented little thermodynamic data base), Kagakugijutsusha, 1985.
[5] R.N. Singh, J. Am. Ceram. Soc. 59 (1976) 112.
[6] T. Terai, T. Yoneoka, H. Tanaka et al., J. Nucl. Mater. 233–237 (1996) 1421.
[7] T. Yoneoka, T. Terai, Y. Takahashi, J. Jpn. Inst. Metals 60 (1996) 1.